Available online at www.sciencedirect.com
SCIENCE DIRECT®
International Journal of Heat and Mass Transfer 48 (2005) 2013–2022
International Journal of HEAT and MASS TRANSFER
www.elsevier.com/locate/ijhmt

An alternative two-equation turbulent heat diffusivity closure

Michał Karcz *, Janusz Badur

Institute of Fluid Flow Machinery, Polish Academy of Sciences, Fiszera 14, 80952 Gdańsk, Poland

Received 1 September 2004
Available online 25 February 2005

Abstract

The objective of this paper is to present an alternative closure for turbulent heat transport, that has been established on the ground of v^2–f model with so-called elliptic relaxation equation and the two-equation model for turbulent thermal field. New formulae on the eddy heat diffusivity is proposed. Additionally the production term of destruction rate of temperature variance transport equation is reformulated. No damping functions are involved in this model. Results of numerical computation have been compared with the experimental data for fully developed thermal field in the pipe and DNS heat transfer prediction for two-dimensional channel flow. The model predicts reasonably well the near-wall distribution of basic turbulence statistics.

Keywords: Turbulent heat flux; Two-equation model; Turbulent Prandtl number

1. Introduction

The modelling of the turbulent flows with heat transfer focuses mainly on solving properly velocity field rather than temperature field. It is generally accepted that the influence of turbulence models for momentum on the solution is much greater than the influence of turbulence closures for energy equation which are usually simplified to an algebraic expressions. The simplest way of turbulent heat flux modelling by means of employing a constant or varying turbulent Prandtl number Pr_t seems to be sufficient and economical but only for prediction of smooth pipe and simple channel flows without separation. Such a way of turbulent heat flux modelling is a direct succession of the so-called Reynolds analogy between turbulent heat and momentum transfer. Some authors argue that more sophisticated models are needed especially that it should be no more difficult and time consuming [1,2].

In view of present research experience one of the most important problems is connected with proper modelling of the near-wall effects. These effects, which are dominant in the case of flows in channels, pipes and other domains closely constrained by walls, are rather simplified by employing so-called wall or damping functions that are based on the geometry and some flow parameters. Non-local effect of near-wall turbulence as the kinematic blocking ($y^+ < 200$) and the dynamic viscous damping ($y^+ < 20$) could be both alternatively modelled by introducing an elliptic relaxation equation for the redistribution term in the transport equations for turbulent stresses, that was done by Durbin [3]. Eddy diffusivity version of such a model uses as a turbulent velocity scale in the turbulent viscosity formulation some scalar representation of wall-normal stresses $\overline{v'^2}$, instead of standard turbulent kinetic energy k [4–7].

* Corresponding author.
E-mail addresses: mkarcz@imp.gda.pl (M. Karcz), jb@imp.gda.pl (J. Badur).

0017-9310/$ - see front matter
doi:10.1016/j.ijheatmasstransfer.2004.12.006

Nomenclature

$\overline{v}_j$	mean velocity components	y	wall-normal distance
C_μ, C_η, C_ϵ, C_λ, C_p, C_d	model constants	v'	wall-normal velocity fluctuations
f	variable related to the turbulent energy redistribution in the $\overline{v'^2}$ transport equation	α, α_t	molecular and turbulent heat diffusivity
f_μ, f_λ	damping functions of models	δ_{ij}	Kronecker delta
k	turbulent kinetic energy	ϵ	dissipation rate of k
k_θ	temperature variance	ϵ_θ	destruction rate of k_θ
p	mean pressure	ν, ν_t	molecular and turbulent viscosity
Pr, Pr_t	molecular and turbulent Prandtl number	ρ	fluid density
q	heat flux	σ_θ	coefficient for turbulent diffusion of k_θ and ϵ_θ
Re	Reynolds number	τ_m, τ_θ	turbulent velocity and temperature field timescales
S_{ij}	strain rate tensor	θ'	temperature fluctuations
T	mean temperature		

Modelling of the turbulent heat flux evolution equations is still problematic and the reported results are only slightly better than obtained with lower order closures which based on the eddy diffusivity formulation [2,8,9]. Thus two-equation k_θ–ϵ_θ approach to the modelling of the turbulent heat flux is considered in the present study. Some attention is paid to the destruction rate of temperature variance transport equation. Different approaches are generally employed to predict the generation of ϵ_θ [7–12].

Standing on the ground of Durbin's v^2–f model [3,4] and an additional two-equation k_θ–ϵ_θ turbulent heat transfer closure of Deng et al. [11] a new proposition for turbulent heat flux closure is presented here. It assumes that $\overline{v'^2}$ should be also employed in turbulent heat diffusivity formulation. As a result a damping functions are no longer needed. Constants of model have been calibrated and validated on the base of the experiment by Hishida and Nagano of thermal boundary layer development in the pipe [14,15] and DNS heat transfer data by Kasagi et al. for two-dimensional channel flow [16]. The details of the presented line of reasoning can be found in dissertation [17] and the preliminary results in [18]. Possibilities of extension of presented class of models to multiphase flows are discussed in the paper by Bilicki and Badur [19].

2. Coupled v^2–f–$\overline{\theta'^2}$–ϵ_θ model for turbulent thermal field

Two-equation or second-order Reynolds-stress closures are usually employed in the CFD codes. In these codes, the most popular way of computing turbulent heat flux is the well known simplification by introducing the turbulent Prandtl number Pr_t

$$Pr_t = \frac{\nu_t}{\alpha_t}, \tag{1}$$

which directly links turbulent diffusivity of heat α_t with turbulent viscosity ν_t. It is known however, that α_t should be at least represented as a function of turbulent time scales for velocity and thermal fields, which is the main assumption of the two-equation k_θ–ϵ_θ type of closures [2,7–12].

The main concept of a coupled v^2–f–k_θ–ϵ_θ model has been established on the assumption that both turbulent momentum and heat transfer are governed mainly by the turbulent velocity component normal to the wall $\overline{v'^2}$ [3,4]. The normal Reynolds stress component represented here by scalar $\overline{v'^2}$ is naturally damped in the wall vicinity. It could be used as a turbulent velocity scale instead of turbulent kinetic energy k in the eddy diffusivity of heat formulation (3) in an analogy to the eddy viscosity formula that was given by Durbin (2)

$$\nu_t = C_\mu f_\mu k \tau_m \rightarrow C_\mu \overline{v'^2} \tau_m, \tag{2}$$

$$\alpha_t = C_\lambda f_\lambda k \tau_\theta \rightarrow C_\lambda \overline{v'^2} \tau_\theta. \tag{3}$$

In addition the damping function f_λ could be simply omitted in this case. Turbulent time scale of velocity field τ_m is usually defined as a relation of turbulent kinetic energy k and its dissipation rate ϵ. However, it is not clear what time scale τ_θ should be employed in the formulation (3) for turbulent heat diffusivity [2,9]. Most papers report that the turbulent eddy diffusivity of heat α_t should at least involve dynamic time scale k/ϵ, and thermal field time scale k_θ/ϵ_θ [2,8–12], where temperature variance k_θ is defined as

$$k_\theta = \frac{\overline{\theta'^2}}{2}. \tag{4}$$

As a result α_t may be written in the form

$$\alpha_t = C_\lambda \overline{v'^2} \left(\frac{k}{\epsilon}\right)^l \left(\frac{k_\theta}{\epsilon_\theta}\right)^m, \qquad l + m = 1. \tag{5}$$

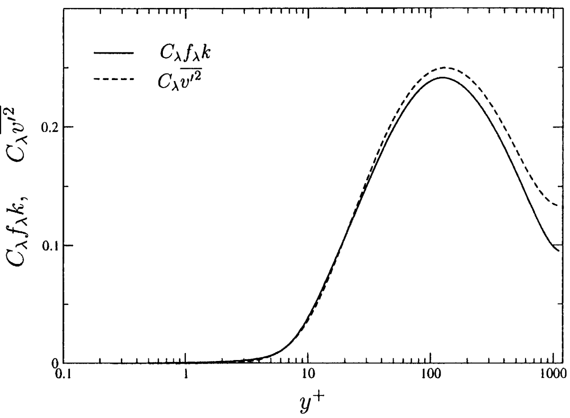

Fig. 1. The wall-normal profiles of $C_\lambda f_\lambda k$, of the Deng et al.'s model and a new proposition $C_\lambda \overline{v'^2}$, of model v^2–f–$\overline{\theta'^2}$–ϵ_θ.

The near-wall profiles of the expression $C_\lambda f_\lambda k$ from original two-equation Deng et al.'s model and proposed $C_\lambda \overline{v'^2}$ from coupled v^2–f–k_θ–ϵ_θ model (Eq. (5)) are presented in Fig. 1.

Employing of new formula $C_\lambda \overline{v'^2}$ instead of $C_\lambda f_\lambda k$ requires only a constant C_λ to be adjusted.

2.1. Model for velocity field

One can find many examples of original and modified v^2–f models [4–7] and also some implementations of an elliptic relaxation method for modelling near-wall effects [20,21]. A full set of governing equations for the v^2–f model is as follows [5,6]:

$$\frac{\mathrm{D}k}{\mathrm{D}t} = \frac{\partial}{\partial x_j}\left[\left(v + \frac{v_t}{\sigma_k}\right)\frac{\partial k}{\partial x_j}\right] + P_k - \epsilon, \tag{6}$$

$$\frac{\mathrm{D}\epsilon}{\mathrm{D}t} = \frac{\partial}{\partial x_j}\left[\left(v + \frac{v_t}{\sigma_\epsilon}\right)\frac{\partial \epsilon}{\partial x_j}\right] + \frac{C_{\epsilon 1}P_k - C_{\epsilon 2}\epsilon}{\tau}, \tag{7}$$

$$\frac{\mathrm{D}\overline{v'^2}}{\mathrm{D}t} = \frac{\partial}{\partial x_j}\left[(v + v_t)\frac{\partial \overline{v'^2}}{\partial x_j}\right] + kf - \frac{\epsilon}{k}\overline{v'^2}, \tag{8}$$

$$f = L^2\frac{\partial}{\partial x_j}\left(\frac{\partial f}{\partial x_j}\right) + \frac{C_1}{\tau}\left[\frac{2}{3} - \frac{\overline{v'^2}}{k}\right] + C_2\frac{P_k}{k}. \tag{9}$$

Eqs. (6)–(9) are solved together with the mean continuity and momentum balance equations

$$\frac{\partial \rho}{\partial t} + \frac{\partial}{\partial x_i}(\rho \bar{v}_i) = 0, \tag{10}$$

$$\frac{\mathrm{D}\bar{v}_i}{\mathrm{D}t} = -\frac{1}{\rho}\frac{\partial p}{\partial x_i} + \frac{\partial}{\partial x_j}\left(v\frac{\partial \bar{v}_i}{\partial x_j} - \overline{v_i' v_j'}\right). \tag{11}$$

After employing the eddy diffusivity concept the unknown turbulent stresses are represented by

$$-\overline{v_i' v_j'} = 2v_t S_{ij} - \frac{2}{3}k\delta_{ij}. \tag{12}$$

The turbulent viscosity is defined by formula (2) and S_{ij} is a strain-rate tensor defined as

$$S_{ij} = \frac{1}{2}\left(\frac{\partial \bar{v}_i}{\partial x_j} + \frac{\partial \bar{v}_j}{\partial x_i}\right), \tag{13}$$

which is also employed to model a production of turbulent kinetic energy P_k

$$P_k = 2v_t S_{ij} S_{ij}. \tag{14}$$

The time and length scales which appear in Eqs. (7) and (9) are as follows:

$$\tau = \max\left[\frac{k}{\epsilon}, 6\sqrt{\frac{v}{\epsilon}}\right], \tag{15}$$

$$L = C_L \max\left[\frac{k^{3/2}}{\epsilon}, C_\eta\left(\frac{v^3}{\epsilon}\right)^{\frac{1}{4}}\right]. \tag{16}$$

The model constants for v^2–f model employed in the present analysis are the same as in [5]

$$\begin{gathered} C_\mu = 0.22, \quad C_1 = 0.4, \quad C_2 = 0.3, \quad C_L = 0.25, \\ C_\eta = 85, \quad C_{\epsilon 2} = 1.9, \quad \sigma_\epsilon = 1.3. \end{gathered} \tag{17}$$

An additional coefficient $C_{\epsilon 1}$ which controls the shear layer spreading rate [3] needs to be computed from:

$$C_{\epsilon 1} = 1.4\left(1 + 0.045\sqrt{\frac{k}{\overline{v'^2}}}\right). \tag{18}$$

The boundary conditions for solid walls ($y \to 0$) are:

$$k = 0, \quad \epsilon \to \frac{2vk}{y^2}, \quad \overline{v'^2} = 0, \quad f \to -\frac{20v^2\overline{v'^2}}{\epsilon y^4}. \tag{19}$$

2.2. Model for thermal field

The Fourier–Kirchhoff energy balance equation has the standard form

$$\mathscr{T}(\theta) = \frac{\mathrm{D}\theta}{\mathrm{D}t} + \frac{\partial}{\partial x_j}\left(\alpha\frac{\partial \theta}{\partial x_j}\right) = 0. \tag{20}$$

A so-called Reynolds averaging procedure of Eq. (20) allows to obtain the mean energy equation

$$\frac{\mathrm{D}T}{\mathrm{D}t} = \frac{\partial}{\partial x_j}\left(\alpha\frac{\partial T}{\partial x_j} - \overline{v_j'\theta'}\right), \tag{21}$$

where θ and θ' are instantaneous temperature and fluctuations of temperature respectively ($\theta = T + \theta'$). Eq. (21) includes term $-\overline{v_j'\theta'}$ that needs closing.

Extensive research in the area of turbulent heat flux modelling has been conducted from algebraic to second-order level. Comprehensive reviews can be found in [7,8]. Successful implementation of two-equation heat flux k_θ–ϵ_θ model was presented firstly in 1988 by Nagano and Kim [2]. A number of modified versions of model k_θ–ϵ_θ have been published afterwards [9–11]. Such modelling requires that two additional transport equations are employed, i.e. the temperature variance k_θ and its destruction (dissipation) rate ϵ_θ. Exact transport equations of the temperature variance and its dissipation rate are derived from particular expressions [7]

$$\overline{\theta'\mathscr{T}(\theta)+\mathscr{T}(\theta)\theta'}=0, \tag{22}$$

$$2\alpha\overline{\frac{\partial\theta'}{\partial x_j}\frac{\partial}{\partial x_j}\mathscr{T}(\theta')}=0. \tag{23}$$

The resulting transport equations have the form [7,11,12,17]

$$\begin{aligned}\frac{D\overline{\theta'^2}}{Dt}=&\underbrace{\frac{\partial}{\partial x_j}\left(\alpha\frac{\partial\overline{\theta'^2}}{\partial x_j}\right)}_{D_\theta}-\underbrace{\frac{\partial}{\partial x_j}\left(\overline{v'_j\theta'^2}\right)}_{D^t_\theta}-\underbrace{2\overline{v'_j\theta'}\frac{\partial T}{\partial x_j}}_{P_\theta}\\&-\underbrace{2\alpha\overline{\frac{\partial\theta'}{\partial x_j}\frac{\partial\theta'}{\partial x_j}}}_{\epsilon_\theta},\end{aligned} \tag{24}$$

for temperature variance k_θ and

$$\begin{aligned}\frac{D\epsilon_\theta}{Dt}=&\underbrace{\frac{\partial}{\partial x_k}\left(\alpha\frac{\partial\epsilon_\theta}{\partial x_k}\right)}_{D_{\epsilon_\theta}}-\underbrace{\alpha\frac{\partial}{\partial x_k}\left(\overline{v'_k\frac{\partial\theta'}{\partial x_j}\frac{\partial\theta'}{\partial x_j}}\right)}_{D^t_{\epsilon_\theta}}\\&-\underbrace{2\alpha\overline{\frac{\partial\theta'}{\partial x_j}\frac{\partial\theta'}{\partial x_k}}\frac{\partial\overline{v}_k}{\partial x_j}}_{P^{\mathrm{M}}_{\epsilon_\theta}}-\underbrace{2\alpha\overline{\frac{\partial v'_k}{\partial x_j}\frac{\partial\theta'}{\partial x_j}}\frac{\partial T}{\partial x_k}}_{P^{\mathrm{T}}_{\epsilon_\theta}}\\&-\underbrace{2\alpha\overline{\frac{\partial v'_k}{\partial x_j}\frac{\partial\theta'}{\partial x_j}\frac{\partial\theta'}{\partial x_k}}}_{P^t_{\epsilon_\theta}}-\underbrace{2\alpha\overline{v'_k\frac{\partial\theta'}{\partial x_j}}\frac{\partial^2T}{\partial x_k\partial x_j}}_{P^{\mathrm{G}}_{\epsilon_\theta}}\\&-\underbrace{2\alpha\overline{\left(\frac{\partial^2\theta'}{\partial x_k\partial x_j}\right)^2}}_{\epsilon_{\epsilon_\theta}},\end{aligned} \tag{25}$$

for destruction rate of temperature variance, ϵ_θ.

The modelling of temperature variance equation k_θ usually bases on the ground of gradient hypothesis for the turbulent diffusion D^t_θ and also for the production terms P_θ

$$D^t_\theta=-\frac{\partial}{\partial x_j}\left(\frac{\alpha_t}{\sigma_\theta}\frac{\partial k_\theta}{\partial x_j}\right), \tag{26}$$

$$P_\theta=\alpha_t\frac{\partial T}{\partial x_j}\frac{\partial T}{\partial x_j}. \tag{27}$$

Transport equation of temperature variance takes thus a final form

$$\frac{Dk_\theta}{Dt}=\frac{\partial}{\partial x_j}\left[\left(\alpha+\frac{\alpha_t}{\sigma_\theta}\right)\frac{\partial k_\theta}{\partial x_j}\right]+P_\theta-\epsilon_\theta. \tag{28}$$

More attention is needed when the destruction rate of temperature variance transport equation is to be considered. The source terms in evolution equation of ϵ_θ (25) include several time and generation-rate scales [7,11,12]. Therefore, it is difficult to find a simple physical interpretation for all of correlations between velocity and temperature fluctuations. The turbulent diffusion term is approximated similarly to Eq. (29) by

$$D^t_{\epsilon_\theta}=-\frac{\partial}{\partial x_j}\left(\frac{\alpha_t}{\sigma_\theta}\frac{\partial\epsilon_\theta}{\partial x_j}\right). \tag{29}$$

Total production rate of ϵ_θ consists of mean gradient production terms $P^{\mathrm{M}}_{\epsilon_\theta}$ and $P^{\mathrm{T}}_{\epsilon_\theta}$, gradient production $P^{\mathrm{G}}_{\epsilon_\theta}$ and turbulent production $P^t_{\epsilon_\theta}$ [8]. The turbulent production term $P^t_{\epsilon_\theta}$ is often omitted or added to mean-field generation processes although it could be important in high-Re-number flows [12]. Only a number of closures involve gradient production term $P^{\mathrm{G}}_{\epsilon_\theta}$, among them the model of Nagano and Kim [2], and also that of Shikazono and Kasagi [9]. The latter involves normal velocity fluctuations $\overline{v'^2}$ and thermal time scale k_θ/ϵ_θ in the expression which approximates gradient production term

$$P^{\mathrm{G}}_{\epsilon_\theta}=2\alpha C_{w2}\overline{v'^2}\frac{k_\theta}{\epsilon_\theta}\left(\frac{\partial^2T}{\partial y^2}\right)^2, \tag{30}$$

where coordinate y is taken as a normal to the wall.

Mean gradient mechanical $P^{\mathrm{M}}_{\epsilon_\theta}$ and thermal $P^{\mathrm{T}}_{\epsilon_\theta}$ production terms are usually approximated separately [2,9,10,12]. Deng et al.'s model employs one term only, which blends mechanical and thermal contribution by means of mixing time scale and thermal production rate P_θ [11]

$$P^{\mathrm{M+T}}_{\epsilon_\theta}=C_{p1}f_{p1}\sqrt{\frac{\epsilon\epsilon_\theta}{kk_\theta}}P_\theta. \tag{31}$$

Following Deng et al.'s proposition, in the present model one term is assumed that approximates all generation sources of ϵ_θ. Let us consider situation when coefficients $l=m=0.5$ in new eddy diffusivity expression (5) as in standard models [2,10,11]. Then introducing formula (5) together with production term (27) to Eq. (31) one can obtain a simplified approximation of mean gradient terms $P^{\mathrm{M}}_{\epsilon_\theta}$ and $P^{\mathrm{T}}_{\epsilon_\theta}$

$$P^{\mathrm{M+T}}_{\epsilon_\theta}=C_{p1}\overline{v'^2}\left(\frac{\partial T}{\partial x_j}\right)^2, \tag{32}$$

that is close in its form to $P^{\mathrm{G}}_{\epsilon_\theta}$ gradient production term of Shikazono and Kasagi (Eq. (30)).

Dissipation of ϵ_θ is modelled as in many two-equation turbulent heat flux closures [2,9–12] but without using any damping functions. Finally, transport equation of ϵ_θ takes the following form:

$$\begin{aligned}\frac{D\epsilon_\theta}{Dt}=&\frac{\partial}{\partial x_j}\left[\left(\alpha+\frac{\alpha_t}{\sigma_{\epsilon_\theta}}\right)\frac{\partial\epsilon_\theta}{\partial x_j}\right]+C_{p1}\overline{v'^2}\left(\frac{\partial T}{\partial x_j}\right)^2\\&-C_{d1}\epsilon_\theta\frac{\epsilon_\theta}{k_\theta}-C_{d2}\epsilon_\theta\frac{\epsilon}{k}.\end{aligned} \tag{33}$$

The model constants are determined on the base of existing two-equation closures [2,8–11]. Constant C_λ which appears in the eddy diffusivity relation is estimated by comparison of new expression $C_\lambda\overline{v'^2}$ and $C_\lambda f_\lambda k$ from previous model by Deng et al [11]. Similar procedure is to be employed (together with some calibration) for the production term in ϵ_θ equation. The destruction terms constants are assumed identical to [8,10,11] as their impact on the solution is rather weak [7]. It should be remembered that the transport equations in the present study are constructed on the base of k_θ rather than $\overline{\theta'^2}$. As a consequence some attention is needed when different closures constants are compared. In summary, the constants of a implemented two-equation model, are taken as follows:

$$C_\lambda = 0.2, \quad C_{p1} = 0.63, \quad C_{d1} = 1.0, \quad C_{d2} = 0.9, \quad l = 1.5, \quad m = -0.5, \quad \sigma_\theta = 1.0. \tag{34}$$

The boundary conditions on the impermeable walls has been assumed identical to standard two-equation closures [10,11]

$$k_\theta = 0, \quad \epsilon_\theta \to \alpha\frac{k_\theta}{y^2}. \tag{35}$$

Additionally for cases with constant heat flux at the wall (q_w = const.) a new boundary conditions proposed by Deng et al. could be validated

$$k_\theta = 0, \quad \frac{\partial\epsilon_\theta}{\partial y} = 0. \tag{36}$$

It is known, that for case of constant heat flux, temperature fluctuations are not zero at the wall, especially when unsteady heat conduction processes in solid walls are considered [13]. However in an air flow (molecular Prandtl number $Pr = 0.71$) the wall temperature fluctuations are negligibly small [22], so assumption of vanishing k_θ at the walls could be employed.

The model with boundary conditions represented by (35) and the model that employs (36) for approximation of ϵ_θ at the wall will be called *ver. 1* and *ver. 2* respectively.

3. Computation results

Validation of combined model could be conducted with standard references data, i.e. the experiment of Hishida and Nagano of developed thermal field in the heated pipe with the uniform temperature at the wall (T_w = const.) [14,15] and DNS results of Kasagi for a heated 2D channel with the uniform heat flux imposed at the wall (q_w = const.) [16].

3.1. Numerical procedure

A commercial CFD code FLUENT 6.0.12 [23], based on the finite volume method, was used to solve the set of scalar Eqs. (6)–(9) for the velocity field and (28)–(33) for the thermal field together with mean continuity (10), momentum (11) and energy (21) equations.

All six equations of combined model were implemented into the solver by an external subroutine [17]. The QUICK spatial scheme was employed to discretize convection terms of the mean momentum and energy balance equations. The second-order discretization scheme was applied for the convection terms of scalars evolution equations. The diffusion terms for all equations were central-differenced. The SIMPLEC method was used for pressure–velocity coupling. For both pipe and 2D channel cases a structured grids were built with proper exponential near-wall refinement.

At the beginning, the standard value $Pr_t = 0.85$ was employed to solve the energy balance equation. When solution of four equations describing turbulent velocity field became converged, the next two equations, i.e. for temperature variance and its destruction rate, were implemented and involved in turbulent eddy diffusivity formulation (5), instead of using the turbulent Prandtl number concept (1).

In addition a low-Reynolds-number k–ϵ model for turbulent velocity field of Abe et al. [10], that is available in FLUENT 6.0.12 [23], has been employed together with implemented by the external subroutine closure of Deng et al.'s for comparison.

3.2. Heated pipe flow (T_w = const.)

Numerical solution has been compared with experimental data given in [14,15]. The experiment of heated pipe, by means of uniform temperature at the wall, was performed in air flow ($Pr = 0.71$) for a Reynolds number $Re = 40{,}000$ based on the pipe diameter and bulk velocity. The results of calculations have been presented for cross section where flow was fully developed.

The profiles of mean velocity v^+ are presented in Fig. 2. Model $\overline{v'^2}$–f predicts the velocity profile reasonably well when compared to experimental data and Abe et zal. low-Re-number model. Slight overprediction of velocity is noticed in the region of $y^+ \gtrsim 100$. The same problem is reported in [4] for similar set of constants of v^2–f model.

The predicted mean temperature T^+ normalized by friction temperature is plotted in Fig. 3. Again the results computed by means of coupled model described here as *ver. 1* correlate well with the experimental and modelled data by Deng et al.'s closure.

The profiles of normalized temperature variance k_θ^+ are presented in Fig. 4. The shape of the modelled curves is similar to experimental data but some overprediction of k_θ^+ value is observed. Differences between coupled and Deng et al.'s closures are however small.

The changes of the production of temperature variance P_θ^+ are depicted in Fig. 5.

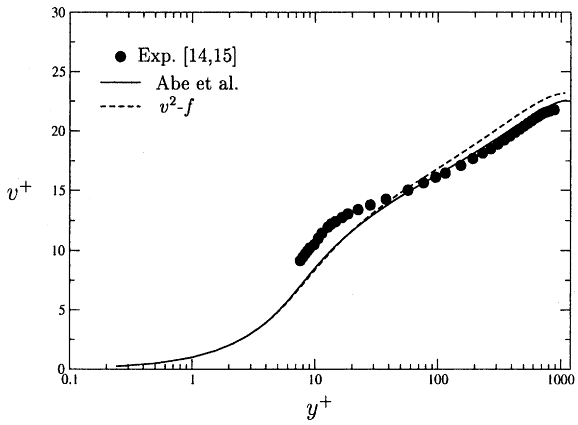

Fig. 2. Mean velocity v^+ profile (T_w = const.).

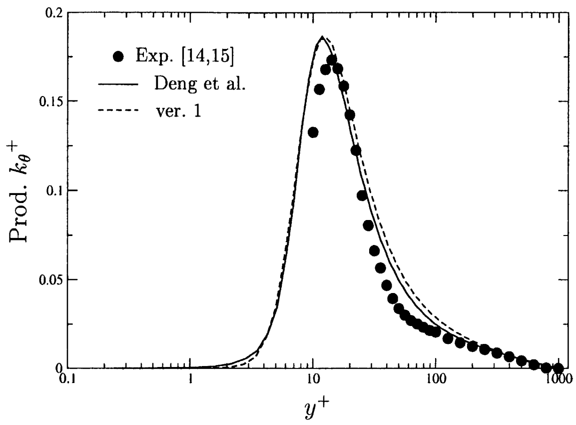

Fig. 5. Production of the normalized temperature variance P_θ^+ (T_w = const.).

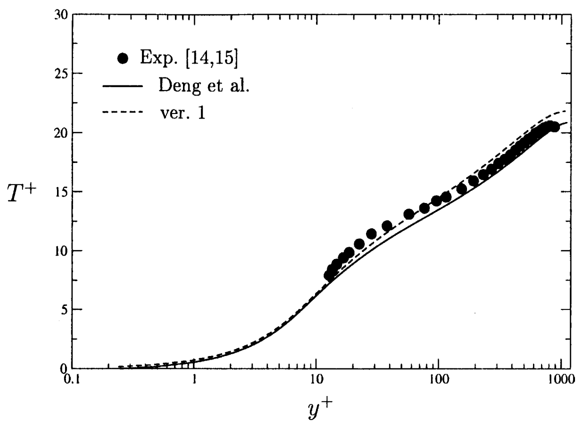

Fig. 3. Profile of mean temperature T^+ (T_w = const.).

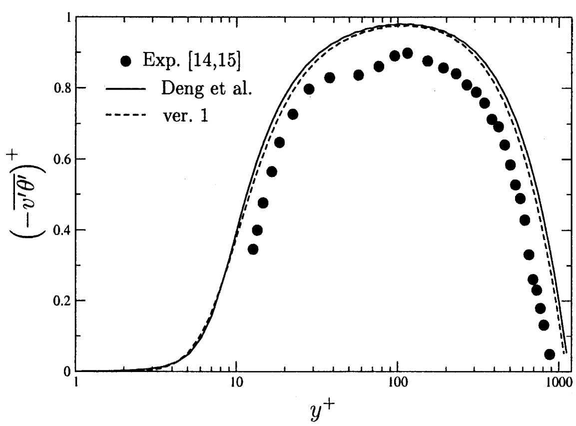

Fig. 6. Turbulent heat flux $(-\overline{v'\theta'})^+$ (T_w = const.).

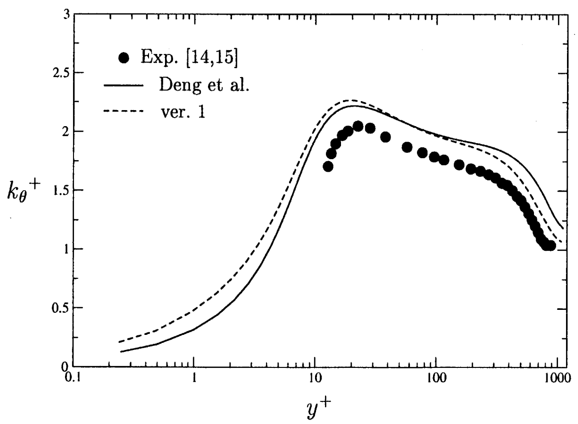

Fig. 4. Changes of temperature variance k_θ^+ (T_w = const.).

The predicted non-dimensional turbulent heat flux $(-\overline{v'\theta'})^+$ is illustrated in Fig. 6. As in the case of temperature variance (Fig. 4) and its production rate (Fig. 5) results are in good agreement with measurements. Both models employed in the analysis give almost the same results.

Changes of the measured and computed turbulent Prandtl number are presented in Fig. 7. Additionally, the Kays and Crawford [1] correlation for Pr_t is plotted for comparison. The results obtained with the combined v^2–f–$\overline{\theta'^2}$–ϵ_θ model correlate quite successfully with the experimental data and Kays formulae.

3.3. Heated channel flow (q_w = const.)

Following Deng et al.'s suggestion on using different expression to approximate ϵ_θ value at the wall for the case of uniform heat flux imposed at the wall, two kinds of boundary condition were investigated. First of them (described as *ver. 1*) employs, for evaluation of ϵ_θ at the wall, formula (35)—the same as in the analysis with

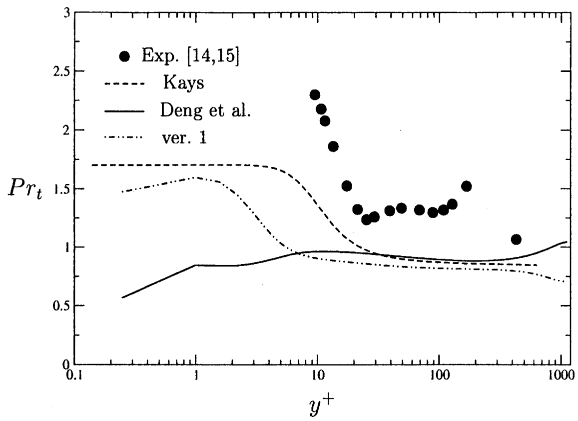

Fig. 7. Profile of the turbulent Prandtl number Pr_t for the case of (T_w = const.).

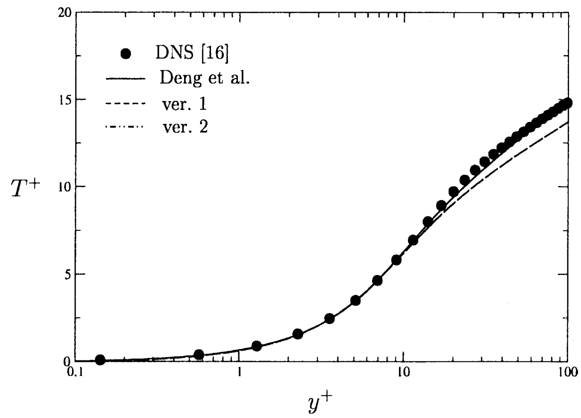

Fig. 9. Profile of mean temperature T^+ for channel flow (q_w = const.).

constant temperature at the wall of heated pipe presented in Section 3.2. Second (described below as *ver. 2*) uses new formula (36) that was derived for constant heat flux at the wall.

The reference data base on DNS results of Kasagi et al. [16] for two-dimensional heated channel flow $Re = 4560$ (based on channel half width) of air ($Pr = 0.71$) as the working medium. Durbin's v^2–f model was validated by the comparison of velocity profiles in boundary layer which is presented in Fig. 8. A good agreement is observed between DNS and computed data both for Abe et al. and v^2–f models.

Temperature profile for 2D channel flow is shown in Fig. 9. Here some underprediction of temperature is observed for both versions of coupled closure. On the other hand, the model of Deng et al. exactly predicts temperature profile from DNS data.

The corresponding comparison of temperature variance and its dissipation rate are presented in Figs. 10 and 11, respectively. The maximum level of temperature

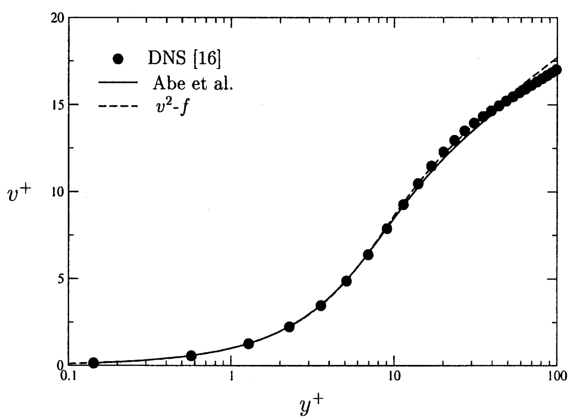

Fig. 8. Profile of mean velocity v^+ in 2D channel flow.

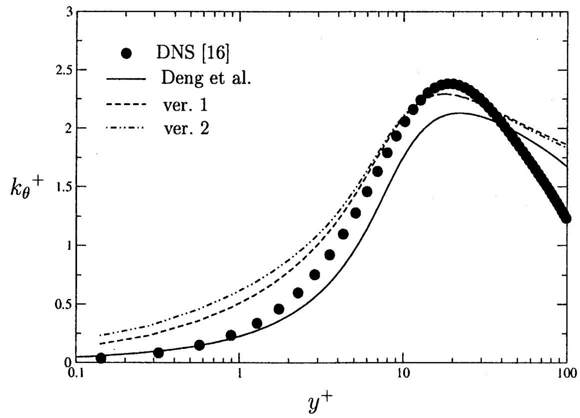

Fig. 10. Near-wall changes of temperature variance k_θ^+ (q_w = const.).

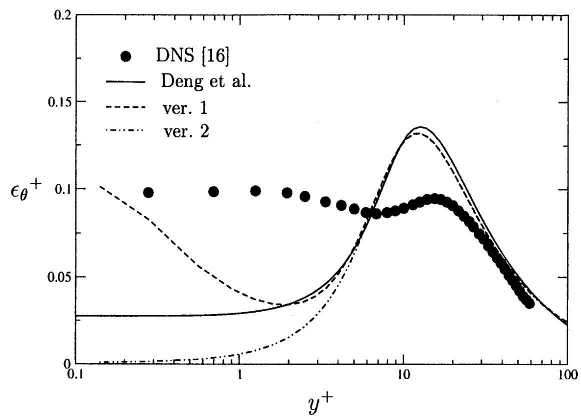

Fig. 11. Destruction rate of temperature variance ϵ_θ^+ (q_w = const.).

fluctuation intensity is predicted correctly by coupled models but the slope of the computed curves is too low when compared to DNS data. However predicted values seem to be slightly better than those obtained with Deng et al. model.

The predictions of ϵ_θ^+ obtained with coupled closures are as accurate as those from the Deng et al.'s model for $y^+>5$. The best results are obtained with *ver. 1* of coupled model where computed destruction rate at the wall is equal ϵ_θ from DNS. However, when condition $\partial\epsilon_\theta/\partial y = 0$ is employed with the coupled model (*ver. 2*) then ϵ_θ attains too low value at the wall.

The turbulent Prandtl number Pr_t profiles in the wall vicinity are shown in Fig. 12. The computed results of Pr_t are in some opposition to data of Kasagi where turbulent Prandtl number approaches an asymptotic value $\sim$1 at the wall. The results by means of Deng et al.'s model are below DNS data and coupled models generally overpredict DNS data in the near-wall region $y^+ < 10$. When condition $\partial\epsilon_\theta/\partial y = 0$ is employed with coupled model (*ver. 2*) then Pr_t reaches extremely high value at the wall. Similar results were reported in [22] for higher molecular Prandtl number $Pr \gg 1$.

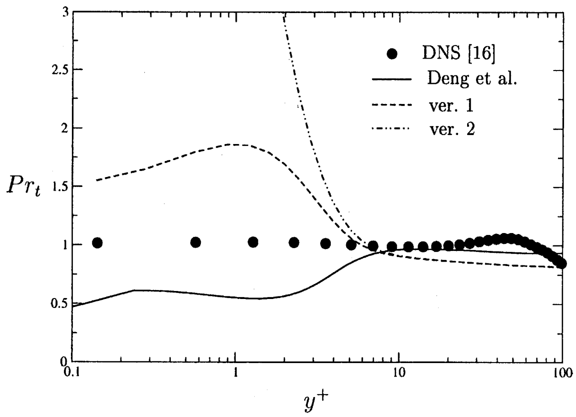

Fig. 12. Profile of turbulent Prandtl number Pr_t in thermal boundary layer (q_w = const.).

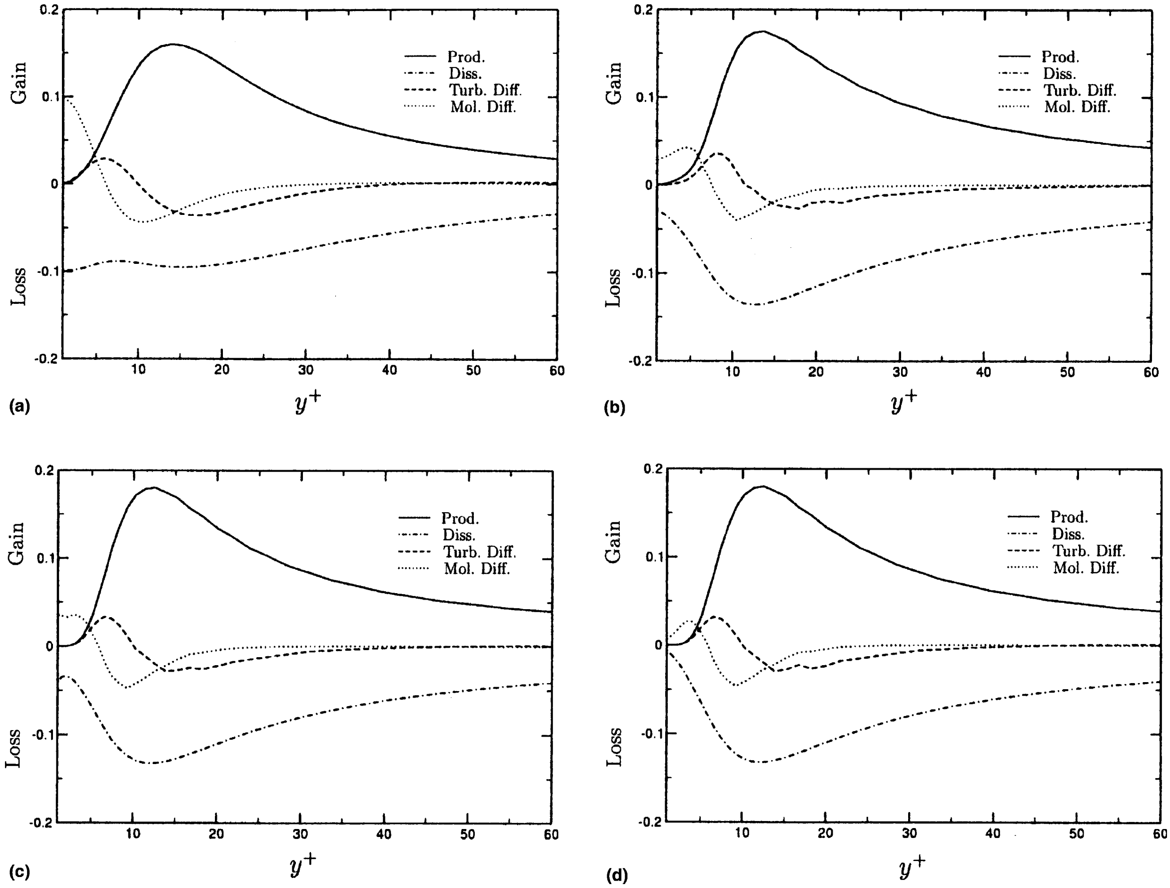

Fig. 13. Budget of the temperature variance k_θ: (a) DNS results by [16], (b) Deng et al.'s model, (c) *ver. 1* closure, (d) *ver. 2* closure.

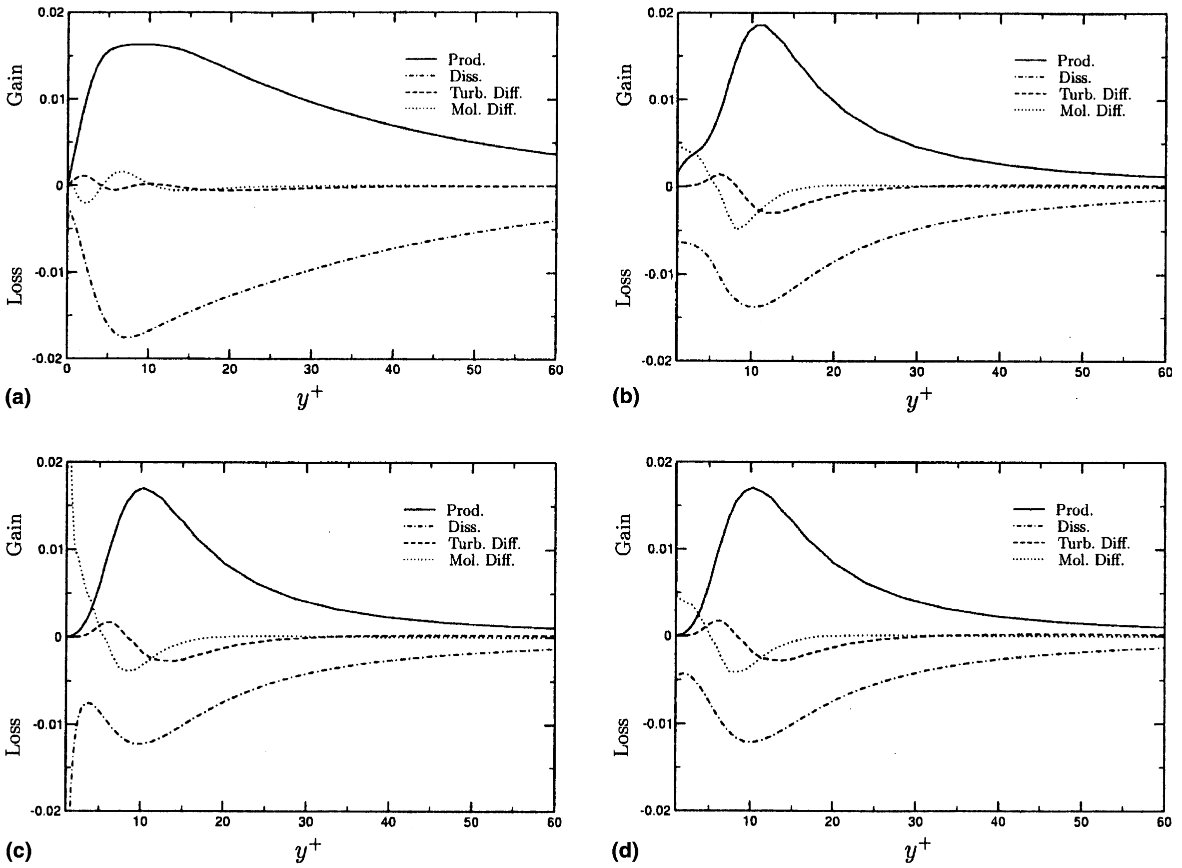

Fig. 14. Budget of the destruction rate of temperature variance ϵ_θ: (a) DNS results by [16], (b) Deng et al.'s model, (c) *ver. 1* closure, (d) *ver. 2* closure.

The budgets of temperature variance k_θ and the relevant destruction rate ϵ_θ are presented in Figs. 13 and 14, respectively. Results for all investigated models are close to the DNS predictions in the case of k_θ budgets. The only differences in Fig. 13 are observed in the near-wall dissipation of k_θ. They are connected mainly with type of employed boundary condition at the wall.

More discrepancies are revealed in Fig. 14. The production of ϵ_θ from DNS prediction is much greater than computed with all models despite the fact that the maximum value is predicted rather correctly. The computed changes of dissipation of ϵ_θ are lower than DNS results and no one model is better. These discrepancies reveal that a more carefully modelling of production and dissipation source terms of ϵ_θ should be considered.

4. Concluding remarks

The two-equation eddy diffusivity concept for both velocity and thermal fields is a simple and reliable way to obtain fast and correct solutions for engineering applications. As it was reported earlier, v^2–f model handles fairly well the separation flows [4–6], where dissimilarity exists between velocity and temperature fields [10]. Two-equation turbulent heat flux modelling avoids the turbulent Prandtl concept that is in such situations deficient [1].

Presented v^2–f–k_θ–ϵ_θ model seems to be comparable with the standard low-*Re*-number models coupled with the known two-equation turbulent heat flux closures. The advantage of presented closure results mainly from the proper non-local near-wall modelling as in original model implemented by Durbin [4], where no geometrical damping functions have to be employed. Employing thermal time scale τ_θ and normal velocity fluctuations $\overline{v'^2}$ for turbulent diffusivity of heat evaluation (5) makes the coupled model more consistent. The changes of mean flow and turbulent heat flux quantities in the wall proximity are predicted successfully for analysed cases.

It should be pointed, however, that more attention is needed when the source terms of ϵ_θ are investigated. In view of predicted results, especially for near-wall profile and the budget of ϵ_θ, all the processes which are responsible for generation and dissipation should be properly accounted for.

References

[1] W.M. Kays, Turbulent Prandtl number—Where are we?, ASME J. Heat Transfer 116 (1994) 284–295.

[2] Y. Nagano, C. Kim, A two-equation model for heat transport in wall turbulent shear flows, ASME J. Heat Transfer 110 (1988) 583–589.

[3] P.A. Durbin, A Reynolds stress model for near-wall turbulence, J. Fluid Mech. 249 (1993) 465–498.

[4] P.A. Durbin, Application of near-wall turbulence model to boundary layers and heat transfer, Int. J. Heat Fluid Flow 14 (1993) 316–323.

[5] R. Manceau, S. Parneix, D. Laurence, Turbulent heat transfer predictions using the $\overline{v^2}$–f model on unstructured grids, Int. J. Heat Fluid Flow 21 (2000) 320–328.

[6] A. Ooi, G. Iaccarino, P.A. Durbin, M. Behnia, Reynolds averaged simulation of flow and heat transfer in ribbed ducts, Int. J. Heat Fluid Flow 23 (2002) 750–757.

[7] C.G. Speziale, R.M.C. So, Turbulence modelling and simulation, in: R.W. Johnson (Ed.), The Handbook of Fluid Dynamics, CRC Press LLC, Boca Raton, Florida, 1998, pp. 14.1–14.111.

[8] Y. Nagano, Modelling heat transfer in near-wall flows, in: B.E. Launder, N.D. Sandham (Eds.), Closure Strategies for Modelling Turbulent and Transitional Flows, Cambridge University Press, Cambridge, 2002.

[9] N. Shikazono, N. Kasagi, Second-moment closure for turbulent scalar transport at various Prandtl numbers, Int. J. Heat Mass Transfer 39 (1996) 2977–2987.

[10] K. Abe, T. Kondoh, Y. Nagano, A new turbulence model for predicting fluid flow and heat transfer in separating and reattaching flows—II. Thermal field calculations, Int. J. Heat Mass Transfer 38 (1995) 1467–1481.

[11] B. Deng, W. Wu, S. Xi, A near-wall two-equation heat transfer model for wall turbulent flows, Int. J. Heat Mass Transfer 44 (2001) 691–698.

[12] T.P. Sommer, R.M. So, Y.G. Lai, A near-wall two-equation model for turbulent heat fluxes, Int. J. Heat Mass Transfer 35 (1992) 3375–3387.

[13] T.P. Sommer, R.M. So, H.S. Zhang, Heat transfer modeling and the assumption of zero wall temperature fluctuations, ASME J. Heat Transfer 116 (1994) 855–863.

[14] M. Hishida, Y. Nagano, Structure of turbulent velocity and temperature fluctuations in fully developed pipe flow, ASME J. Heat Transfer 101 (1979) 15–22.

[15] Y. Nagano, M. Tagawa, Statistical characteristics of wall turbulence with passive scalar, J. Fluid Mech. 196 (1988) 157–185.

[16] N. Kasagi, Y. Tomita, A. Kuroda, Direct numerical simulation of passive scalar field in a turbulent channel flow, ASME J. Heat Transfer 114 (1992) 598–606.

[17] M. Karcz, Performance analysis of the thermal diffusers and its application to the gas turbine cooling, PhD thesis, Institute of Fluid-Flow Machinery Polish Academy of Sciences, Gdańsk, 2003.

[18] M. Karcz, J. Badur, A turbulent heat flux two-equation $\overline{\theta'^2}$–ϵ_θ closure based on the $\overline{v^2}$–f turbulence model, TASK Quart. 7 (2003) 375–387.

[19] Z. Bilicki, J. Badur, A thermodynamically consistent relaxation model for turbulent binary mixture undergoing phase transition, J. Noneq. Therm. 28 (2003) 145–172.

[20] M. Wacławczyk, J. Pozorski, J.-P. Minier, Probability density function computation of turbulent flows with a new near-wall model, Phys. Fluids 16 (2004) 1410–1422.

[21] V. Wizman, D. Laurence, M. Kanniche, P.A. Durbin, A. Demuren, Modelling near-wall effects in second-moment closures by elliptic relaxation, Int. J. Heat Fluid Flow 17 (1996) 255–266.

[22] N. Kasagi, A. Kuroda, M. Hirata, Numerical investigation of near-wall turbulent heat transfer taking into account the unsteady heat conduction in the solid wall, ASME J. Heat Transfer 111 (1989) 385–389.

[23] FLUENT User's Guide, Fluent Inc., Lebanon, USA, 2002.